



A machine learning-based surrogate model to approximate optimal building retrofit solutions

Emmanouil Thrampoulidis ^{a,b,*}, Georgios Mavromatidis ^c, Aurelien Lucchi ^d, Kristina Orehouning ^b

^a EEH-Power Systems Laboratory, Swiss Federal Institute of Technology (ETH), Zürich, Switzerland

^b Laboratory for Urban Energy Systems, Empa Dübendorf, Switzerland

^c Group for Sustainability and Technology, Swiss Federal Institute of Technology (ETH), Zürich, Switzerland

^d Institute for Machine Learning, Data Analytics Lab, Swiss Federal Institute of Technology (ETH), Zürich, Switzerland

HIGHLIGHTS

- Machine learning-based surrogate model to predict near-optimal retrofit solutions.
- Validated with a conventional building simulation-optimization model.
- Case study reveals good accuracy, ease of application and computational efficiency.
- Convenient for non-expert decision makers due to small set of input data.
- The model is scalable and applicable for retrofit analyses in wide-areas.

ARTICLE INFO

Keywords:

Building retrofit
Energy efficiency
Surrogate model
Machine learning
Multi-objective optimization
Pareto-optimal

ABSTRACT

The building sector has the highest share of operational energy consumption and greenhouse gas emissions among all sectors. Environmental targets set by many countries impose the need to improve the environmental footprint of the existing building stock. Building retrofit is considered one of the most promising solutions towards this direction. In this paper, a surrogate model for evaluating the necessary building envelope and energy system measures for building retrofit is presented. Artificial neural networks are exploited to build up this model in order to provide a good balance between accuracy and computational cost. The proposed model is trained and tested for the case study of the city of Zurich, in Switzerland, and is compared with one of the most advanced models for building retrofit that uses building simulation and optimization tools. The surrogate model operates on a smaller input set and the time required to derive retrofit solutions is reduced from 3.5 min to 16.4 usec. Results show that the proposed model can provide significantly reduced computational cost without compromising accuracy for most of the retrofit dimensions. For instance, the retrofit costs and the energy system selections are approximated with an average accuracy of $R^2 = 0.9408$ and $f1\ score = 0.9450$, respectively. Finally, yet importantly, such surrogate retrofit models may effectively be used for bottom-up retrofit analyses for wide areas and can contribute towards accelerating the adoption of retrofit measures.

1. Introduction

1.1. Background

According to the European Commission, operational energy involved in the building sector is responsible for nearly 40% and 36% of the total energy consumption and CO₂ emissions, respectively [1]. According to

the Swiss Federal Office of Energy, the same percentages apply also for Switzerland [2]. Thus, reducing the environmental footprint of the building sector is a big step towards a more sustainable environment.

The need to improve the energy efficiency of the building sector seems to be well understood in the policy-making community. This has led to the establishment of building energy-saving targets both at country- and continental-level. For instance, in Switzerland the Swiss energy strategy 2050 [3] has been legislated. In Europe energy-saving

* Corresponding author at: Laboratory for Urban Energy Systems, Empa, Überlandstrasse 129, 8600 Dübendorf, Switzerland.

E-mail address: Emmanouil.Thrampoulidis@empa.ch (E. Thrampoulidis).

Nomenclature	
<i>General Abbreviations</i>	
Abbreviation	Full description
ANNs	Artificial Neural Networks
ASHP	Air Source Heat Pump
CHP	Combined Heat and Power
CPU	Central Process Unit
CRP	Conventional Retrofit Process
DMs	Decision Makers
ECMs	Energy Conservation Measures
EH	Energy Hub
EPS	Expanded Polyesterene
GAs	Genetic Algorithms
GEAK	Gebäudeenergieausweis der Kantone (Building energy certificate of Swiss cantons)
GHG	Greenhouse Gas
GIS	Geographical Information Systems
GSHP	Ground Source Heat Pump
GWR	Eidgenössische Gebäude- und Wohnungsregister (Federal Register of Buildings and Dwellings)
KBOB	Koordinationskonferenz der Bau- und Liegenschaftsorgane der öffentlichen Bauherren (Coordination conference of the building and real estate authorities for the building owners)
MFH	Multi-Family House
MILP	Mixed Integer Linear Programming
ML	Machine Learning
PF	Pareto Front
PFP	Pareto Front Point
ReLU	Rectified Linear Unit
PV	Photovoltaics
SFH	Single Family House
TP	True Positive
SIA	Swiss Society of Engineers and Architects
UBEM	Urban Building Energy Modeling
CHF	Swiss Franc
En. Carrier	Energy Carrier
<i>Variables</i>	
Variable	Full description
<i>U-Value</i>	Thermal transmittance
α	Significance level of hypothesis test
p-value	Probability of observing a test statistic as extreme as, or more extreme than, the observed value under the null hypothesis
λ	Regularization parameter
C	Total number of classes
R^2	Coefficient of determination
d	Continuous output of conventional retrofit process
o	Continuous output of surrogate retrofit model
P	Total number of outputs
k	Optimization objective index
f	Objective function
i,j	Pareto front point indices

targets are established by the Energy Performance of Buildings Directive [4], its amendment [5], and its most recent directive with a strong focus on building retrofit [6]. To achieve those targets, in other words to reduce the energy consumption and emissions of the building sector, several steps are needed.

One of the main goals of the Energy Performance of Buildings Directive is that all new buildings should be nearly zero-energy buildings by 2020. This can be considered as a necessary but not sufficient step towards reducing the environmental impact of buildings. The use of advanced and efficient energy models, to provide the appropriate construction measures that can guarantee an efficient and sustainable building operation, can eventually lead to nearly zero energy buildings [7]. However, the construction of new efficient buildings only ensures the stability of the current energy consumption and greenhouse gas (GHG) emissions without being able to reduce them. The European building stock, as stated in [1], includes many buildings (35%) that are over 50 years old, and the retrofit rate is less than 1.2% per year. In Switzerland, in particular, the retrofit rate is still below 1% [8]. Moreover, many of those buildings are under a historical protection status, while demolition and rebuilding is not a financially attractive option for others. Consequently, in order to reduce energy consumption and GHG emissions, special focus should be given on the existing building stock. Building retrofit is one of the most promising solutions towards this direction.

Building retrofit typically refers to both demand- and supply-side interventions; the first pertaining to interventions on the building envelope, for instance by enhancing the thermal insulation of a building's walls, and the second to energy system replacements. The latter includes suggestions on building-level (decentralized) energy system technologies, e.g., heat pumps, but also on district-level (locally centralized) energy system solutions, e.g., centralized heat pump that can serve several buildings. It also includes suggestions on integration of renewable energy technologies and the necessity of energy storage.

Even though building-specific retrofit solutions are of great

importance, they should be part of a coordinated large-scale retrofit plan, e.g., to develop city-wide energy retrofit strategies. This is also suggested, in [9], after a thorough review of the available retrofit decision support methodologies, to benefit from: (i) a balanced responsibility and involvement of various stakeholders, i.e., municipality, building owners, and policy makers, (ii) a more systematic and effective approach to derive energy policies, strategies and incentives that can facilitate the wider adoption of retrofit solutions and, (iii) the advantages of locally centralized-supply technologies. Centralized-supply technologies or else district-level solutions have certain advantages compared to decentralized ones, such as better efficiencies and emission profiles due to lower losses, more efficient operation and lower maintenance costs and easier renewable technologies integration. However, when several constraints exist, building level solutions might be preferable. In any case, both building-level and district-level solutions should be evaluated before the decision process.

Building retrofit covers a large range of interventions, also called energy conservation measures (ECMs), which increase both the complexity of the problem and the solution space. Due to the various complex, heterogeneous and highly dependent specialties involved in the building sector, and to many competing criteria that have to be satisfied in order to interconnect the various ECMS, building retrofit is considered a highly challenging and building-specific task [10], typically performed by energy consultants. Those consultants are usually equipped with the appropriate engineering tools so as to be able to provide retrofit solutions to the decision makers (DMs), e.g., building owners, renters, in a quite reasonable time. However, it is a fact that ECMS have not been endorsed that much by DMs, due to asymmetry of information that consequently leads to uncertainties in cost and energy savings [11]. Even though there exist open-access engineering models, which can be used by DMs, expertise is needed to run them so as to come up with optimal ECMS. Moreover, even though those models are accurate, they become computational expensive when the problem space is increased, as for instance when a building retrofit analysis must be

performed for a whole district, or city. The goal of this paper is to present a surrogate retrofit model that provides a good balance between accuracy and computational cost, while also using inputs that are known or easily accessible by DMs. For this purpose, machine learning (ML) algorithms, and more specifically artificial neural networks (ANNs), are used to train this surrogate model. The proposed approach is illustrated using as a case study the city of Zurich, in Switzerland.

1.2. Related work

The process of building retrofit consists of several steps. Data-collection is usually the first step of this process. It is influenced by building specific and external factors [10] and it might involve the use of heterogeneous building information, e.g., census, 3D building, and weather data, among others, that are not always available. The second step, the backbone of this process, is the building retrofit analysis. It might pertain to compiling a list of candidate measures and the comparison of their performance. The last step is the selection of the most appropriate retrofit measure from the DMs. In this section, the related work focusing on building retrofit analysis is discussed.

1.2.1. Engineering models for building retrofit analysis

Several engineering models have been presented for the building retrofit analysis process. These models vary in complexity and accuracy. Usually, the more complex the model is, the more accurate the results are and the more computational resources are needed. This is because there is a huge variety of ECMs that have to be investigated. One of the simplest and maybe the fastest retrofit process uses steady state building performance calculations. More specifically, the energy demand of a building is calculated for different ECMs and this is used as a criterion to select the best performing ECM. Ceballos-Fuentealba et al. [12] combined such steady state linear energy equations with an easy to tune parameter optimization algorithm to support decisions on building envelope interventions for non-residential buildings. More advanced retrofit processes are based on the use of dynamic building performance simulation tools such as EnergyPlus [13]. Those tools are capable of evaluating the energy performance efficiency of a small set of ECMs by using dynamic physical models. Other retrofit models, e.g., [14–20] combine building simulation with optimization tools, so as to derive global- or near-optimal solutions by exploring a wider range of ECMs.

One of the most commonly used optimization tools used for building retrofit, are Genetic Algorithms (GAs) that exist in many variations. GAs have been widely used since they can be easily coupled with building simulation tools. GAs are considered to be metaheuristic evolutionary algorithms developed as an attempt to mimic naïve evolution, or in other words to mimic the procedure of mitosis and reproduction, towards an optimum set of solutions [21]. Fan and Xia [14] used GAs to solve the multi-objective optimization problem of deciding on building envelope interventions. The objectives set by the authors were to maximize the energy savings and the net present value, while minimizing the payback period. Ascione et al. [15] developed a GAs approach, combined with building simulation, to derive cost optimal retrofit solutions given a certain budget. The objectives used in this study were the primary energy consumption required by air-conditioning systems and the percentage of annual hours characterized by thermal discomfort. The same methodology but with different objectives and case studies was applied later on in [16]. Similarly, Niemelä et al. [17] developed a combined simulation and GAs optimization to determine cost-optimal retrofit combinations for a large apartment building. This was done by using different sets of objectives; primary energy consumption net present value in a 30 years long life cycle cost analysis and CO₂ emissions. Juan et al. [18] combined GAs with an hierarchical process to assess the current building condition and suggest optimal retrofit actions based on cost and quality.

Another dominant optimization method used in the retrofit process is mixed integer linear programming (MILP) [19]. Even though it is

challenging to couple MILP with building simulation, it outperforms GAs in terms that it can guarantee the global optimality of resulted solutions. One of the existing variations, that involves the use of an urban building energy modeling (UBEM) tool [22], and a multi-objective optimization model, called energy hub (EH) [23] has been successfully applied for providing building envelope and energy system retrofit measures [20]. In this work, this method is used to collect the necessary data to train the surrogate model and to validate its performance. It is referred as conventional retrofit process (CRP). UBEM enables the calculation of energy demand profiles for buildings at urban scale based on building archetypical assumptions for various retrofit measures. The EH is, as defined in [19], "a scalable framework for integrated modeling and optimization of the interactions between multiple energy carriers, and energy conversion and storage technologies within an energy system, but also between multiple systems through different energy networks". Thus, the EH model can be used to propose a set of optimal retrofit solutions, called a Pareto front (PF). Each solution can provide certain building retrofit dimensions, such as the building envelope intervention and the energy system's selection and sizing. For this purpose MILP is used to guarantee global optimality of the suggested retrofit solutions.

There exist many other optimization algorithms used for building retrofit. For instance, a variation of the knapsack problem, which involves combinatorial optimization, is used by Rogeau et al. [24], in combination with steady state calculations, in order to identify cost-optimal demand- and supply-side retrofit solutions. A comprehensive review on optimization algorithms used for existing buildings is given in [25,26].

1.2.2. Building retrofit models using machine learning

ML is nowadays nearly everywhere in our daily life, from the spam filtering to aircraft scheduling and autonomous vehicles. Especially in the energy sector, ML plays an important role. It has been widely used to predict energy demand profiles [27], to improve wind and solar predictions [28], as well as forecast the production from installed photovoltaics or wind turbines [29]. Moreover, they have also been successfully used for fault detection [30,31] as well as for predicting the energy markets' behavior [32] or fuel prices [33]. A comprehensive list of ML applications in the energy sector, and especially neural networks, can be found in [34,35].

Exploiting ML into the building retrofit process is a relatively new direction. Using measured data to train a ML model for building retrofit sounds a promising approach. However, it is very challenging to obtain measured retrofit data and usually such data are subjective and not optimal. For instance, Marasco and Kontokosta [36], trained a classifier to select the optimal ECMs given a set of building characteristics. The data used for training were collected from different energy consultants that subjectively proposed ECMs for various buildings. This led to non-uniform data that demanded an extensive preprocessing and certainly affected the validity and the reliability of the collected data.

That is why most of the existing studies in literature focus on incorporating ML in some parts of the engineering based retrofit approach. Most of the studies couple ML with optimization models to replace the expensive building simulation part. Magnier and Haghhighat [37] were the first to integrate ANNs with GAs optimization, a hybrid optimization problem, for building design. Based on their approach ANNs are trained to predict the building's energy demand. Those demands are then fed into a GAs in order to evaluate potential solutions. The outcome is a PF of design solutions based on two objectives, total energy consumption and average absolute Predicted Mean Vote - thermal comfort. Asadi et al. [38] extended this methodology for building retrofit. Artificial data, created by the authors, were used for single and multi-objective optimization so as not only to derive optimal selection of envelope or system retrofit, but also to understand the influence of the different building design variables. The objectives set by the authors were the energy consumption and the retrofit costs. A similar work was recently published by Ascione et al. [39]. It differs from the previous

studies in that a simultaneous energy system and envelop optimization is considered. The objectives are the energy consumption and the discomfort hours. Moreover, a sensitivity analysis is initially performed in order to reduce the inputs of the ANNs used for building simulation purposes. Furthermore, their approach is developed for an office building but it can be applied to any type of building, as claimed by the authors.

GA-based retrofit solutions usually demand many expensive building energy simulations [25]. In order to reduce the number of expensive simulations, Prada et al. [40] developed a method that combines meta-models, e.g., support vector machines, with GAs to derive retrofit PF. Gilan and Dilkina [41] use active learning Gaussian process coupled with GAs for building design optimization. Active learning is used to reduce the number of samples needed to train a model to predict the building's energy demand. This results to a faster approach compared to simulation-optimization methods that use other predictive models. The drawback of this approach is that no evaluation metric is used to measure its reliability compared to the other studies. Yuan et al. [42] also used Gaussian process, as meta-model, to calculate energy demand profiles for different retrofit scenarios, which are then used by a cost-effectiveness analysis to rank the various retrofit scenarios. A comprehensive review on mixed ML and GAs retrofit methods is provided in [25].

The main drawback of the most of the abovementioned studies is twofold. Firstly, even though the computational time is being considerably reduced, expertise is still needed to run the GA and secondly there is a lack of reliability since GA cannot guarantee optimality [25]. Moreover, some of the main reasons that such multi-objective optimization methods are not widely used is due to extensive calculations times and the lack of user-friendliness [43]. In this context, the contribution of the proposed surrogate model is given in the next subsection.

1.3. Novelty and contribution of the proposed surrogate model

The added value of the proposed surrogate model, which is build up with ANNs to predict building retrofit solutions for residential buildings in the city of Zurich, is fourfold.

First of all, the proposed surrogate model is able to predict retrofit solutions with a substantially reduced computational cost. Engineering building retrofit approaches might involve building simulation and optimization models that can get computationally intensive depending on the level of detail of the building model and the energy systems considered. Indeed, as observed in [44] most of the currently existing building retrofit suffer from long data input and simulation run time.

Secondly, a small set of known or easily accessible building data are used as inputs to the surrogate model. Building retrofit engineering models usually demand a huge array of input data which is challenging to obtain. Even in building databases is quite usual to have missing or wrong data. As a result, DMs can find themselves in a quandary about how to further proceed with retrofitting their buildings. The proposed surrogate model has a relatively small array of input data, e.g., building floor area, construction year, that makes it handier to be used by DMs. Furthermore, the model structure is quite flexible allowing DMs to select the desired optimal solution to be predicted based on their requirements. For instance, if a DM is interested only in the cost-optimal solution he can simply specify it to the model's input.

Thirdly, we could argue that non-expert users might find this surrogate model easier to use compared to engineering retrofit models, such as the CRP. Engineering retrofit models usually demand a high-level of expertise in order to define the appropriate inputs, adjust the parameters and run them. On the other hand, the developed surrogate model has certain usability advantages. Firstly, as soon as the model is trained by experts for given city, there is no need for any further adjustments to run it. Secondly, a smaller and easily accessible building data set is used as input that makes the building data collection process easier. Finally, due to shorter running times and computational cost such a surrogate model

can be beneficial as a mobile building retrofit advisor once trained for a given city.

Lastly, the surrogate model provides a very good balance between accuracy and computational cost that makes it scalable. It can be effectively used for bottom-up building retrofit analyses for wide-areas, such as districts and cities. That means it can predict almost optimal retrofit solutions with a substantial decrease in computational cost and time. Building retrofit in wide areas is very challenging due to computational cost. As argued in [45], the larger the area of investigation the higher are the computational cost and time needed to collect the different data and run the process. The principled generalization ability provided with the use of ANNs to build the model ensures that the model can be directly applied to many residential buildings in the given city so us to derive near-optimal solutions with less computational time and cost. Thus, such a surrogate retrofit model can contribute towards accelerating the adoption of retrofit measures.

1.4. Structure

The paper is structured as follows: In Section 2, the data collection process and the case study used to showcase the proposed surrogate model are described. The development process of the surrogate model is presented in detail in Section 3. In Section 4, the results are illustrated and discussed. Finally, Section 5, provides an overview and the concluding remarks of this work, as well as directions for future research.

2. Data collection and case study

In the following subsections the data collection process and the case study used to collect the data and to showcase the surrogate model are described.

2.1. The Zurich case study

Residential buildings from the city of Zurich (map in Fig. 1), are used as a case study. Zurich is located in the north-central Switzerland and has approximately 435.000 inhabitants. It is the largest city in Switzerland and is divided in 12 districts. Zurich is the capital of canton Zurich that has approximately 225.000 residential buildings.

The proposed surrogate model for building retrofit is developed for Zurich case study. This implies that the model can be successfully used to any of the residential buildings belonging to the city of Zurich in order to calculate near-optimal retrofit solutions. However, it can also be applied to any other city with similar building characteristics. The data collection process applied to this case study was performed with the use of CRP. It is depicted in the diagram shown in Fig. 1 and described in the following subsections.

2.2. Data extraction from building databases

Geographical Information Systems (GIS) and census data were collected from swisstopo and the eidgenössische Gebäude- und Wohnungsregister (GWR) [46] for all residential buildings of the city of Zurich. The collected data involve continuous parameters, such as building's height and floor area, as well as categorical features, such as the energy carrier currently used for the building's heating needs. An ArcGIS model was developed to extract the necessary building features. The building features collected for this work and the respective sources are shown in Table 1.

2.3. Building selection

In order to select the buildings to construct the training data set, three conditions were set. The selected building data set should: (a) be large enough to be used for ML training purposes, (b) consist of all buildings in a selected district, and (c) be representative of the whole

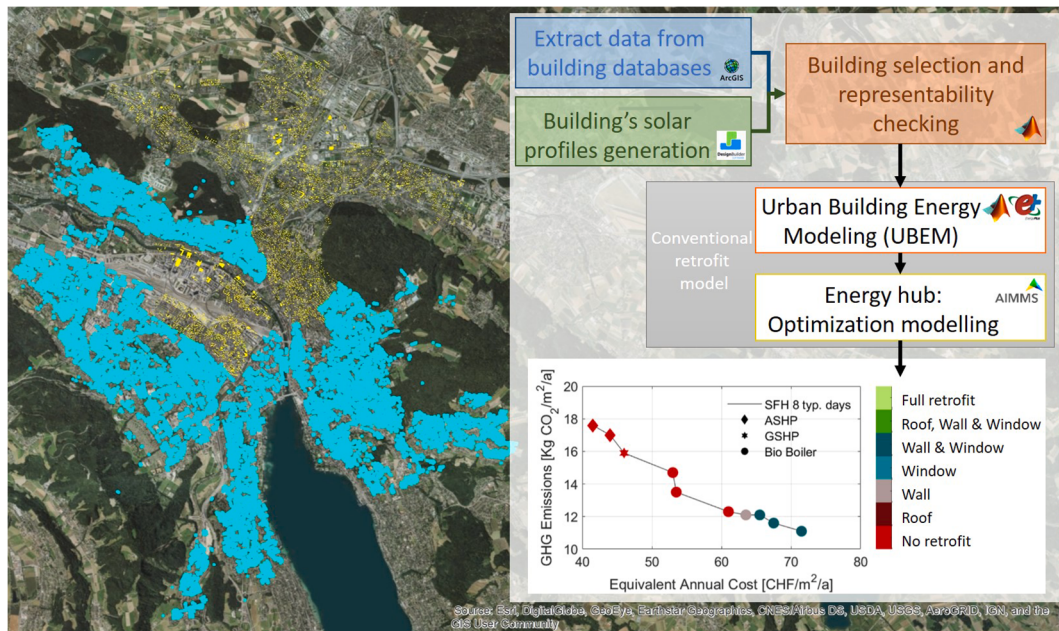


Fig. 1. Zurich map of the selected buildings (cyan dots) of the overall residential buildings (yellow dots) (left). Diagram of the conventional retrofit process (right) used to calculate retrofit solutions for the selected buildings.

Zurich's residential building stock. For ML models, and especially ANNs, the bigger the training data set the better usually is the accuracy. However, the bigger the training data set, the more expensive is the collection of the data. Thus, the data set size selected was a trade-off between the achieved accuracy and the computational cost of collecting the data set. The second condition implies that the building selection was done by selecting whole districts instead of selecting spatially random buildings. This is helpful so as the data of this study can be used as case studies for future work. Therefore, we tested all the possible combinations of districts and we selected the ones that satisfy conditions one and three.

In order to satisfy condition three, we perform a two sample Kolmogorov-Smirnov test for some of the most important continuous building data; the building's construction year, the building's type, the

heating energy carrier, the ground floor area and the building's compactness. The null hypothesis is that the data from the buildings selected (12,806 residential buildings) are from the same continuous distribution of the building data of all residential buildings in the city of Zurich, for which we have available data. The null hypothesis is conducted at the 5% significance level ($\alpha = 0.05$), meaning that there is a 5% risk of concluding that a difference exists when there is no actual difference. The p-value is the probability of obtaining an effect as extreme as, or more extreme than, the one in the actual sample data by assuming that the null hypothesis is true. If the p-value is lower or equal to the α -value, then the null hypothesis is rejected and the selected data do not come from the same distribution of the data of all residential buildings in the city of Zurich. In Fig. 2, the cumulative distribution functions for some categorical and continuous building data for both the

Table 1
Building features collected from the Zurich case study and their corresponding sources.

Features	Source					Calculated
	GWR [46]	3D database [47]	GEAK [48]	KBOB [49]	UBEM [22]	
Building type	x					
Construction year	x					
Ground floor area	x					
Energy carrier	x					
Glazing ratio					x	
Building height	x					
Roof area for PV						From roof slope and floor area
Roof slope	x					
Roof orientation	x					
Embodied emissions of energy systems and building envelope interventions (nominal values)				x		
Insulation costs* (nominal values)			x			
Solar radiation profiles on roof tops						From Zurich weather file and roof slope and orientation
Building coordinates	x					

* Insulation costs include both materials' and installation's costs.

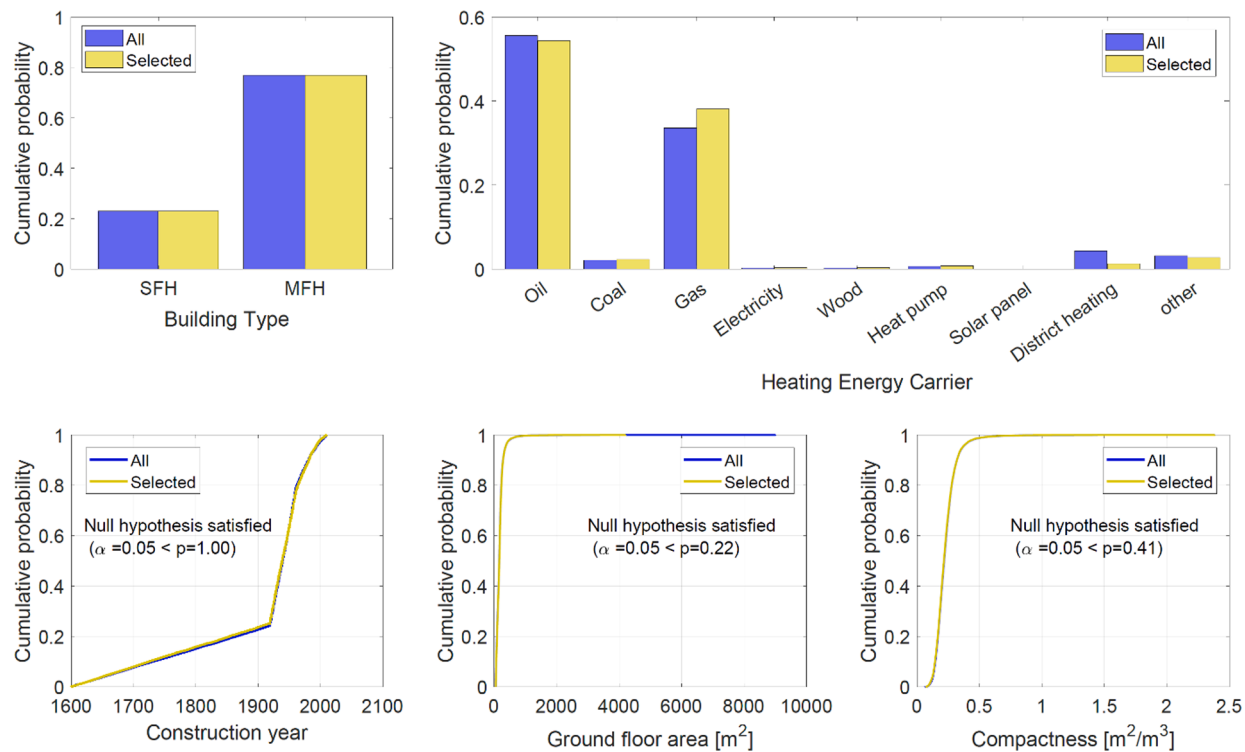


Fig. 2. Cumulative distribution functions for categorical (top) and continuous building data (bottom) for selected (mustard color) and all residential buildings of the city of Zurich (blue color). The Kolmogorov-Smirnov test is used to verify the representability of the selected training data set at the 95% confidence level.

selected and all residential buildings of the city of Zurich are illustrated. We observe that we have a relatively good representation of the involved building types and heating energy carriers in the selected buildings data set compared to the overall building data-set. For the construction year, the ground floor area and the compactness of the selected buildings we conclude that the p-value is higher than the α -value. This implies that, at the 95% confidence level, we fail to reject the null hypothesis. Therefore, we can argue that the null hypothesis is satisfied or in other words the selected data set is a representative set of all the buildings data set.

2.4. Buildings' solar profile generation

The roof inclination and the sun-facing roof area of each building have been calculated by ArcGIS models using the building 3D databases. Moreover, incoming radiation patterns are required to estimate the energy generated by thermal and photovoltaic technologies. The radiation patterns were calculated, in DesignBuilder [50], for different roof inclinations and orientations for a simple building without considering any external shading. Those radiation patterns are stored in a lookup table that is used to match each building with the respective radiation profile based on its roof inclination and orientation.

2.5. Urban building energy modeling

UBEM is used in order to calculate energy demand (heating and electricity) profiles for the following building envelope intervention scenarios:

- Envelope intervention 1:** No retrofit
- Envelope intervention 2:** Roof retrofit
- Envelope intervention 3:** Wall retrofit
- Envelope intervention 4:** Window retrofit
- Envelope intervention 5:** Wall and window retrofit
- Envelope intervention 6:** Roof, wall and window retrofit
- Envelope intervention 7:** Full (roof, wall, window, ground) retrofit

In the context of this paper when referring to retrofitting of building elements we assume an enhancement of the insulation of the respective element in order to reduce its U-value and reach the SIA 380/1 minimal requirements. For instance, wall retrofit implies enhancement of insulation of the walls. Window retrofit implies the change of windows with ones with a better U-value. More details on the U-values and the insulation thicknesses considered can be found in [22].

2.6. Energy hub: Optimization modeling

Usually, in the building retrofit process there exist multiple objectives that have to be satisfied. The most commonly considered dimensions of sustainability in such problems are environmental and economics [26] and as it was shown in an econometric analysis [36], the most important in terms of those two dimensions are the GHG emissions and the involved costs for the proposed improvements, respectively. Those two objectives are considered in this study.

Life Cycle Assessment is usually considered when retrofitting an existing building in order to account not only economic but also environmental impacts. Towards that direction, retrofit and systems embodied emissions were also considered within the EH model. Nominal prices $\left(\frac{\text{CHF}}{\text{m}^2} \right)$ for windows and for different thicknesses of insulation material were derived from [51] while retrofit and system embodied emissions were calculated with values retrieved and processed from [20,49,52–55]. The grid embodied emissions were calculated by interpolating the grid emissions of 2009 and the forecasted emissions for 2050 under the New Energy Policies scenario derived from [55]. All the parameters used to develop the EH model are presented in the Appendix A.

The energy systems, which are necessary to cover the heating demand, considered in the context of this paper are following:

- System 1:** Oil boiler
- System 2:** Gas boiler
- System 3:** Biomass boiler (Bio boiler)

- System 4:** Air-Source Heat Pump (ASHP)
- System 5:** Ground-Source Heat Pump (GSHP)
- System 6:** Oil boiler (existing)
- System 7:** Gas boiler (existing)
- System 8:** Bio boiler (existing)
- System 9:** District heating (existing)
- System 10:** Electricity (existing)
- System 11:** Heat pump (existing)

Systems that are labelled as “existing” refer to the available energy system per building before applying any retrofit. Since there is no information on when the energy systems were installed in the selected buildings, we assumed for existing energy systems to have half the life time of the equivalent new technologies. Furthermore, taking into account the performance degradation of the energy systems, we made the assumption that the existing systems have lower efficiencies compared to the equivalent new technologies. The efficiencies of the energy systems used in this work are based on [19,56] and own assumptions and are presented in the Appendix A.

Except of the necessary energy systems considered to cover the heating demand, solar renewables technologies (photovoltaics – PV, or solar thermal collectors) or energy storages (thermal storage in the form of water tanks and electrical storage in the form of Lithium batteries) can also be selected. It should also be mentioned that the derived hourly energy profiles for the full year for each building envelope intervention scenario are not fed to the Energy Hub model as is, but they are represented with a smaller number of typical day profiles, as referred in [57]. By trying to keep a balance between accuracy and solving time, eight typical days were selected for the EH simulations.

The output of this CRP is a PF consisting of ten optimal retrofit solutions, ranging from the cost- to CO_2 - optimal retrofit solution and some intermediate solutions with different trade-offs between cost and CO_2 emissions. Each PF solution corresponds to different retrofit dimensions such as the system’s selection and sizing, the building envelope intervention and the potential integration and sizing of solar renewables technologies or energy storages.

3. Surrogate model development process

In this paper, a surrogate model for deriving building envelope and energy system retrofit solutions is developed. In Fig. 3, the process followed to develop this model with the use of ML is illustrated. This process enables a good balance between accuracy and computational cost and can be easier used by the DMs since it demands a small set of input data.

As a first step in this development process, all the necessary building and retrofit data from the case study, i.e., the city of Zurich, are collected and stored in a database. The next steps are data pre-processing and the selection of the ML algorithm and the surrogate model’s architecture. The goal is to smoothly and effectively train a surrogate model that can

be run to a set of test buildings so as to come up with a set of near-optimal retrofit solutions, a PF. The PF consists of the cost and the CO_2 optimal solution and some in between solutions. However, before deriving the PF, a data post-processing step is necessary. Those development steps are described in detail in the following subsections.

3.1. Data pre-processing

The next step after collecting the necessary training data is to perform data-preprocessing. This process pertains to outlier detection and feature standardization so as to ensure a reliable training process. For detecting the outliers, isolation forest [58], an unsupervised ML algorithm, was used. The isolation forest algorithm is based on the decision trees concept and it is used for outlier detection in multidimensional feature spaces to split the data to outliers and inliers. One hundred base estimators were used to identify 1281 buildings as outliers. Those buildings were removed from the building dataset. As far as the feature standardization is concerned, normalization was performed for the continuous features, while standardization was applied for the categorical ones. In order to identify the best performing standardization, we fixed the ML model hyperparameters and we tested the training performance for several different methods among which the label, the binary, and the one-hot encoding. The latter had the highest accuracy and it was finally selected. The same procedure was followed for the normalization and among different methods, the quantile normalization according to the 1st and the 3rd quantiles was the best performing one. For standardization the library presented in [59] was used.

3.2. Model architecture and algorithm selection

The following step, after collecting and cleaning the training data set, is to define the architecture of the surrogate model and the ML algorithm to be used. Moreover, the inputs and the outputs of the ML surrogate model have to be defined. During this step special attention is given to the desired characteristics of the surrogate model; namely the reduced complexity, the ease of application and the use of easily accessible building input features by the DMs.

Since the goal of the ML surrogate model is to replicate the functionality of the CRP, the output of both approaches is exactly the same. The output of both processes, as shown in Fig. 4, is a PF consisting of ten optimal retrofit solutions. Each solution has many retrofit dimensions, as already described, and shown in the same figure. The inputs of the surrogate model are fewer than the ones used by the CRP and are selected so as to ensure that they are known or easily accessible by DMs. For instance, the CRP demands as input the embodied emissions and the retrofit costs for the different building envelope interventions. However, such input features are not required in the surrogate model since it is challenging to obtain them. The full set of inputs used in the CRP and the surrogate approaches is depicted in Fig. 4. The blue color represents the continuous features while the red color represents the categorical

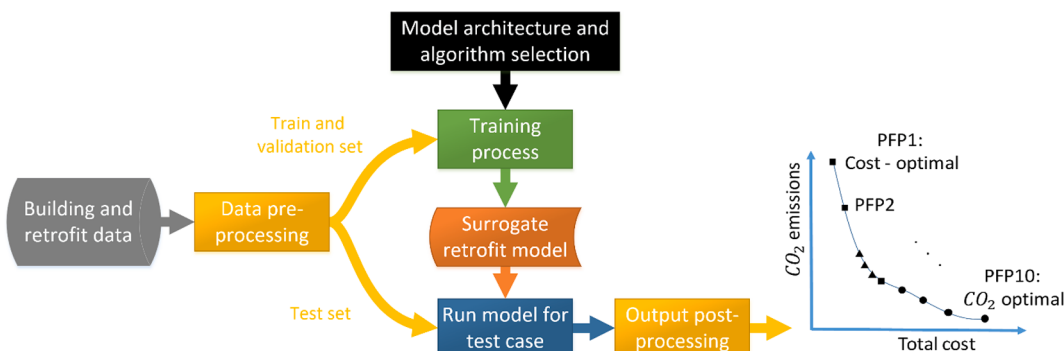


Fig. 3. Steps followed to train and test the surrogate retrofit model to predict the necessary building retrofit solutions (near optimal Pareto front).

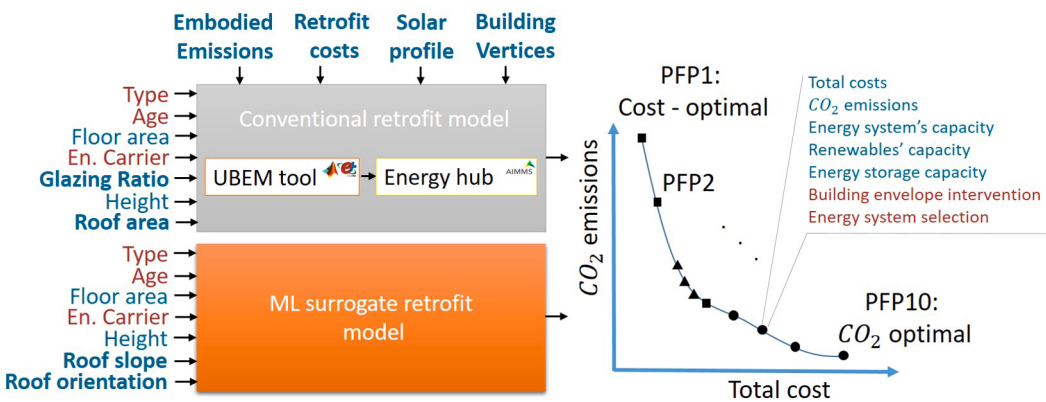


Fig. 4. The proposed surrogate model uses a smaller set of inputs that are known or easily accessible by the decision makers. The blue color represents the continuous features while the red color represents the categorical features. The bolded input features are uniquely used by either the CRP or the surrogate model.

features. The bolded input features are uniquely used by either the CRP or the surrogate model.

The CRP involves the use of complex building simulation and optimization tools that demand as inputs highly heterogeneous data. This approach is capable to understand the nonlinear inter-dependences of those inputs and, with the use of physical models, to derive, global optimal retrofit solutions in a reliable way. The problem complexity is further increased if we consider the dimensionality of the outputs and that both the input and the outputs involve continuous and categorical features. A single ML algorithm could potentially be used to mimic the CRP. This could capture a big share of the problem knowledge; however, in such a case the PF as a whole (with all the different retrofit dimensions) would have to be evaluated, which demands custom cost functions and evaluation metrics that have to be developed. As shown in [60], this approach considerable increases the training time, hindering the main ML advantage which is the fast training process with the use of simple cost functions and evaluation metrics. Therefore, the problem of deriving a PF of retrofit solutions is divided into two smaller simpler subproblems.

In Fig. 5, the structure of the ML surrogate model is depicted. It is

divided into two sub-models; the first is the prediction of the CO₂-optimal solution while the second one is the prediction of the rest of the solutions composing the PF. For the prediction of the CO₂-optimal solution, which is the Pareto front point (PFP) 10 solution, we use a ML model that has as inputs the building features, depicted in Fig. 4, and the implicit solution number N we want to predict, in this case $N = 10$. The next step, is to predict the remaining PFPs' solutions. This is done by using another ML model which has the same inputs plus the previously calculated ($N + 1$)th PFP solution. For instance, if we want to predict the $N = 9$ th solution we will use as input the calculated retrofit solution of 10th solution which is the CO₂-optimal solution. In that way, the prediction starts from the CO₂-optimal solution and moves towards the cost-optimal solution. The main reason for breaking down the problem of predicting in once the PF into the one of predicting the PFPs separately, is to benefit from a simpler training process. Moreover, such an approach enables a better and more precise parameter tuning and handling of the learning process so as to achieve a better performance. Finally, by breaking down the generation of the PF solutions a more flexible retraining process might be followed. For instance, if there is a

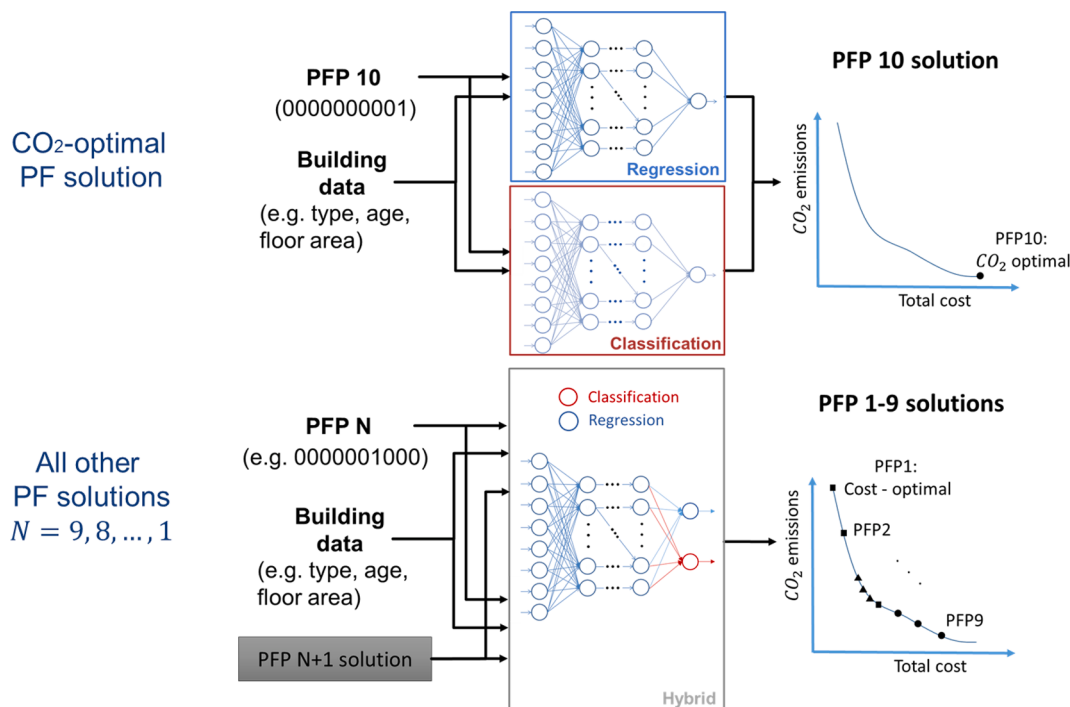


Fig. 5. Structure of the proposed surrogate retrofit model. Two machine learning sub-models are developed; one for the CO₂ optimal solutions and one for the rest of the Pareto front solutions.

need to retrain the model for the cost-optimal solutions then only one part of the surrogate model will be affected.

The final step is to select the ML algorithm to build the two ML sub-models needed to predict the PF of near-optimal retrofit solutions. As already mentioned the problem in question involves the use of both continuous and categorical variables and thus a ML algorithm that can predict both at once would be the best selection. Even though there exist many ML algorithms in the literature, it could be argued that they are case specific and thus there are no rules of thumbs on how to select the appropriate algorithm and it is suggested that different ones should be tested. Some algorithms are dedicated to regression, such as ridge regression, others to classification problems, such as Naive Bayes classifier, while others can work for both types of problems, such as ANNs and random forests. Both ANNs and random forest could be a good alternative for this work. However, ANNs were preferred since they have been widely and successfully used in the energy and building sector [61]. ANNs have been originated as an attempt to mimic the capability of the human brain neurons to process and handle huge amount of data so as to perform specific complex tasks. The latest ANNs developments can be found in [58]. In the context of this work, we use feedforward ANNs in which information flows from input to the output and there are no feedback connections. Three different feedforward ANNs are employed, regressor ANN for predicting continuous variables, classifier ANN for categorical variables and hybrid ANN. Hybrid ANNs are able to predict both continuous and categorical variables from the two nodes of the output layer as can be seen in Fig. 5. Thus, each ML sub-model might consist of one regressor and one classifier or one hybrid ANN. The selection depends on the best performing combination.

3.3. Training process

After having defined the structure and the ML algorithm used to develop the surrogate model, the next step is to define certain parameters to enable an effective training process. This involves not only the definition of the ANNs hyperparameters but also the training parameters and the evaluation metrics to be used to assess the performance of the surrogate model.

Even though ANNs are a very powerful ML algorithm their main disadvantage is that every ANN has several hyperparameters that have to be properly selected in order to ensure a reliable training process. Such hyperparameters that have to be tuned include the number of hidden layers and hidden nodes and the activation function per layer. In order to define those hyperparameters, a grid search was performed with the use of a validation set. That is why, the building dataset is split into training, validation and test set with shares 75%, 15% and 15%, respectively.

Up to three layers and a big set of hidden node combinations is used for the grid search in order to identify the best performing ANN for the two ML sub-models. The various combinations tested are presented in Table 2. For instance, when three hidden layers are selected then one possible combination is 100, 200 and 300 hidden nodes for each of the hidden layers, respectively. For the hidden layers, the Rectified Linear Unit function (ReLU) was used, while for the output layers, the linear and the soft-max activation functions where used for regression and classification, respectively [62].

As far as the training process is concerned, first of all we define the training parameters. This is done by fixing the ANNs hyperparameters and varying the training parameters in order to find the ones that lead to the best training performance. For the batch size, or in other words the number of samples to be propagated through the ANN for each iteration, the optimal number was found to be 850. While the optimal number of epochs, or in other words how many times the entire dataset is passed through the ANN, was found to be 600. Concerning the training algorithm, several were tested, with the best performing being the “Adamax” with its suggested parameters in [63]. The cost functions used were the L2 loss function and the categorical cross entropy with class weighting,

Table 2

Surrogate retrofit model's parameters for the training process. Grid search is used to identify the best performing hyperparameters in terms of the highest validation performance.

Parameter	Value(s)
Hidden layers / nodes	1 / 50, 100, 200, 300, 400, 500 2 / [50,100], [100,150], [128,264], [200,300], [300,400], [400,500] 3 / [50,100,150], [64,128,264], [100,200,300], [200,300,400], [300,400,500]
Activation functions	ReLU (hid. layers) and Linear (reg.), soft-max (class.)
Cost functions	L2 loss with $\lambda = 0.001$ (reg.), categorical cross entropy & class weighting (class.)
Dropout	0.3, 0.5 (Optimized by grid search)
Evaluation metrics	Coefficient of determination R^2 (reg.), f1 score (class.)
Training function	Adamax (parameters as in [63])
Epochs	600 (Optimized by grid search)
Batch size	850 (Optimized by grid search)

for the regressor and the classifier, respectively. Class weighting is necessary so as to prevent the substantial class imbalance appearing in the training data set. For instance, as seen in Fig. 6, there exists a big class imbalance for both building envelope intervention and energy systems selection for PFP1, or else the cost-optimal solution. Class weighting ensures that each Roof instance is treated with the same importance as for example the Window instance.

The regularization parameter as well as the dropout method are used to avoid overfitting. Grid search was performed in order to define the parameters of both regularization techniques. For the L2 loss the regularization parameter is found to be $\lambda = 0.001$ while for the dropout depending on the model the best values were 0.3 and 0.5. In order to evaluate the training process we use, for the categorical variables, the weighted f1score for multi-class problems presented in Equation (1). This weighted f1score for each of the categorical variables is given as the sum of the f1score per class weighted and divided by the true positive (TP) instances per class. The f1score per class is given in Equation (2) as the harmonized mean of precision and recall.

$$f1score = \sum_{class=1}^C TP_{class} * f1score_{class} / \sum_{class=1}^C TP_{class} \quad (1)$$

$$f1score_{class} = 2 * precision_{class} * recall_{class} / (precision_{class} + recall_{class}) \quad (2)$$

The continuous variables are evaluated with the use of the coefficient of determination (R^2). If we assume P outputs, one of the continuous outputs of the CRP as d and the equivalent output of the surrogate model as o, then the coefficient of determination is given from Equation (3).

$$R^2 = \left(\sum_{p=1}^P o_p d_p - \sum_{p=1}^P o_p \sum_{p=1}^P d_p \right) / \left(\sum_{p=1}^P d_p^2 - \sum_{p=1}^P d_p \sum_{p=1}^P d_p \right) \quad (3)$$

Both metrics range between zero and one, with the latter indicating the ideal performance. Finally, Keras [64] with Tensorflow as backend is used to train the surrogate model, and Tensorboard [65] is used to control and ensure a reliable training process. A summary of all the selected parameters is given in Table 2.

3.4. Run model for test case

A small set of buildings, from the case study of Zurich is used in order to test the performance of the surrogate model. More specifically, the trained model is used to predict the PF solutions of those test buildings. This step is necessary so as to both check the generalization ability of the

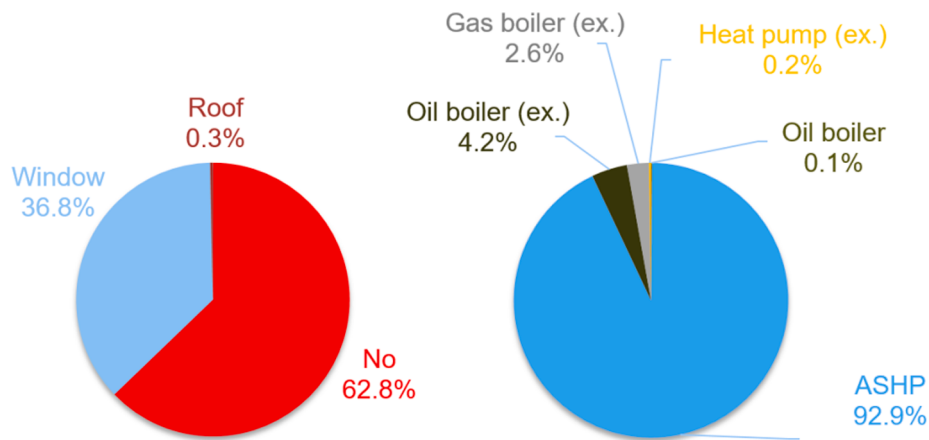


Fig. 6. Class imbalance for PFP1: Cost-optimal solution on training data set for building envelope interventions (left) and energy system selections (right). Class weighting in the cost function is used to handle class imbalance and improve prediction performance.

developed surrogate retrofit model and illustrate the use of such a model.

3.5. Output post-processing

The output of the surrogate retrofit model should replicate the output of the CRP. Thus, the output should be a PF of near-optimal retrofit solutions. In order to ensure that the output is a PF, we have to assure that the predicted PFPs from the ANNs are PF dominant points. In order to achieve that, after training the surrogate model and using the model for prediction, a data-post processing step is necessary. This data-post processing step involves the use of a PF dominant filter that has the functionality shown in Equation (4).

$$\begin{aligned} \text{A PFP } x_i \text{ dominates a PFP } x_j, \text{ with } i \\ \neq j, \text{ if and only if, for each objective } k = 1, 2 : f_k(x_i) < f_k(x_j) \end{aligned} \quad (4)$$

In other words, after combining the outputs of the two ML submodels that form the surrogate retrofit model, we feed the predicted solutions to the abovementioned filter in order to end up with only the PF dominant points. After that, the predicted PF can be compared for

evaluation purposes with the one calculated from the CRP.

4. Results and discussion

In this section, the training results as well as the prediction performance of the surrogate retrofit model for a set of test buildings, are presented and discussed. As already mentioned, the building data-set is divided into three subsets; the training, the validation and the test-set. The first two subsets were used to ensure that the trained model is not overfitting or underfitting, or in other words, to ensure its generalization ability and also to fine-tune the models hyperparameters. The test set is used to confirm the generalization ability and illustrate the prediction performance in a set of test buildings that has never been used in the training process.

4.1. Prediction performance of surrogate model

In Fig. 7, the prediction performance on the test set of residential buildings of the city of Zurich is shown. The performance of the continuous retrofit dimensions, such as the total annual costs and the energy system's capacity, is measured with the use of R^2 which is

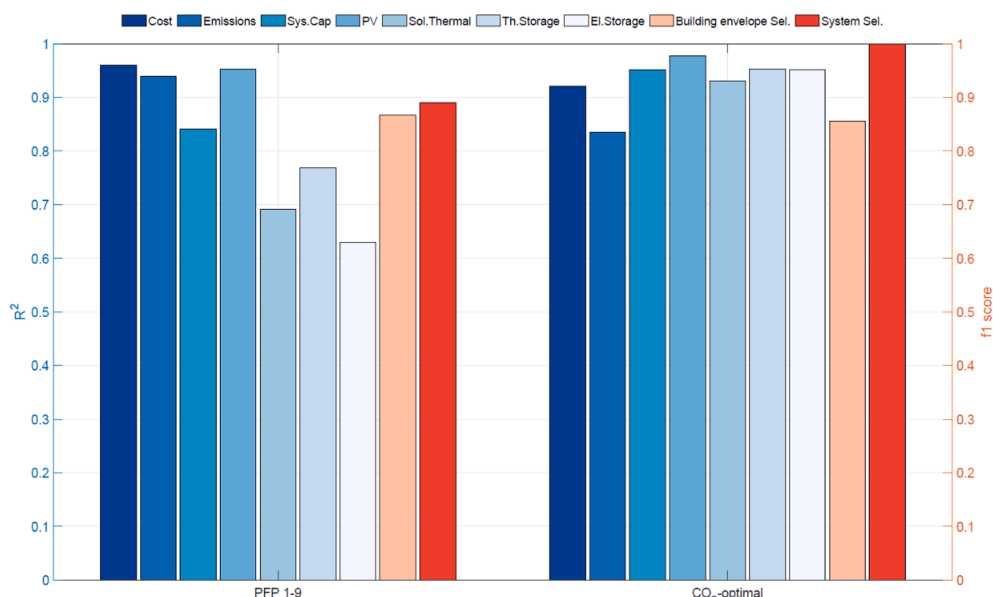


Fig. 7. Prediction performance of the surrogate retrofit model for a test set of residential buildings. The different colors represent the different retrofit dimensions. The continuous retrofit dimensions (blue hue) are evaluated with the coefficient of determination R^2 , while the categorical dimensions (red hue) are evaluated with the f1 score.

represented on the left y-axis. The f1 score is measured on the right y-axis and is used to quantify the performance of the categorical retrofit dimensions, such as the building envelope interventions and the energy system selection. The different colors represent the different retrofit dimensions. More specifically, the blue hue colors represent the continuous variables while the red hue represent the categorical ones.

The test results exhibit a very good prediction performance for the CO₂-optimal solution. This is mainly due to the fact that there is a clear pattern in the training data and especially for the system selection, in which the biomass boiler is almost always selected as the CO₂-optimal solution. For the continuous variables an average $R^2 = 0.9315$ is achieved while an average value of $f1score = 0.9276$ is observed for categorical variables. For the rest of the PFPs, for the continuous variables an average coefficient of determination value of $R^2 = 0.8262$ is observed, while for the categorical variables an $f1 score = 0.8786$, is achieved. Overall, the highest performance is achieved for predicting the PV capacity with an average $R^2 = 0.9650$. Yet, for the other renewable energy technology alternative, which is the solar thermal collectors, an average score of $R^2 = 0.8110$ is observed. The overall average prediction performance on the objective values is $R^2 = 0.9408$ and $R^2 = 0.8867$ for the total annual costs and CO₂ emissions, respectively. For the energy system's capacity installed, an overall average coefficient of determination of $R^2 = 0.8965$ is achieved. The lowest overall average prediction performance is observed for the electrical storage capacity with $R^2 = 0.7910$. This can partially be explained by the fact that the electrical storage is rarely selected in the optimal retrofit solutions due to the high cost of the batteries. Thus, the training set includes few retrofit solutions

that include an electrical storage and eventually there is not enough knowledge given to the surrogate model to predict it. The CO₂-optimal solution is an exemption because the numbers of buildings that are suggested to have an electrical storage is drastically increased. For the other type of storage available, the thermal, an overall average coefficient of determination of $R^2 = 0.8609$ is achieved.

In Fig. 8, the prediction performance of the surrogate model on a set of test buildings for the cost-optimal solution is depicted. Evaluation plots are depicted for some of the continuous and categorical retrofit dimensions. For the continuous variables, we depict the regression plots for the equivalent annual costs, the energy system's capacity and the photovoltaics' capacity. For the depicted continuous variables, we observe a very good accuracy. For instance, for the equivalent annual costs we achieve a coefficient of determination of $R^2 = 0.944$ while for the photovoltaics' capacity an $R^2 = 0.965$ is observed.

In order to illustrate the performance of the surrogate model for the categorical variables, we use a structured visualization, called confusion matrix. In each row, the buildings belonging to a specific true class are depicted, while each columns consists of the buildings belonging to a specific predicted class. The sum of the diagonal values of the confusion matrices represents the number of buildings for which there was a matching between predicted and true class. For example, for 1057 buildings, out of 1728 test buildings, the building envelope intervention was correctly predicted to be no change on the building envelope. However, although for 8 more buildings the true label was no building envelope intervention, the surrogate model suggests a change of the windows with more efficient ones. By summing up the diagonal values

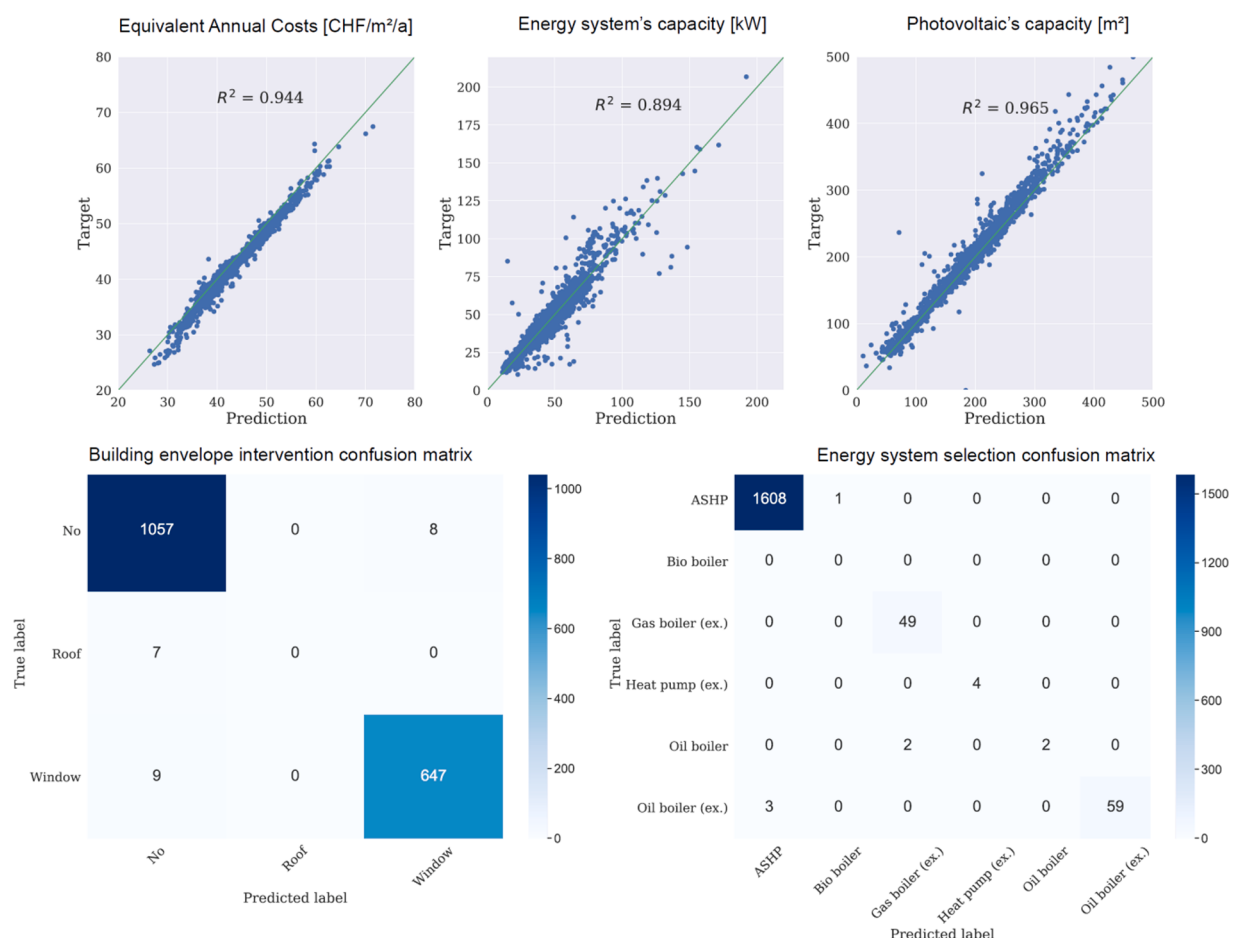


Fig. 8. Prediction performance of the surrogate model on a test set of residential buildings for the Pareto front point 1: Cost-optimal solution. The prediction performance of some of the continuous variables is depicted with regression plots (top) and the categorical variables' prediction performance is illustrated with confusion plots.

and dividing by the overall number of the test buildings in both confusion matrices, we can conclude that for 98.6% and 99.6% of the test buildings, we had a correct prediction for the building envelope intervention and energy system selection, respectively. For PFP5, for which more classes are represented the respective percentages are 0.89% and 0.87% for building envelope interventions and energy systems selection, respectively (Appendix B).

4.2. Prediction of retrofit solutions for residential buildings

In order to illustrate better the performance of the surrogate retrofit model, we used the trained model to predict the PF of some residential buildings of the city of Zurich. The goal is to observe how well we can approximate the output of the CRP for different retrofit dimensions. In Fig. 9, the comparison is performed for three different retrofit dimensions from the left to the right; the building envelope interventions, the energy system selection and their respective capacity, and the selection whether to integrate solar renewable technologies and if this selection should be combined with thermal, electrical or both storage options. The solid line refers to the PF derived from the CRP while the dotted one refers to the output of the surrogate model. The two axes in each of the three plots represent the two objectives used for the optimization process, the equivalent annual costs and the CO_2 emissions.

All the plots in Fig. 9, refer to a MFH, built between 1919 and 1948, with a total floor area of 189.5 m^2 and a height of 15.4 m . The MFH is heated with a gas boiler. For the PF comparison on the left, the building envelope intervention retrofit dimension, the marker colors represent the various building envelope interventions available to choose from. A perfect matching on the prediction of the building envelope interventions is observed for all PFPs except of PFP7. For PFP7 the target intervention is enhancement of wall and roof insulation and change of the windows with more efficient ones, while the prediction is full building envelope interventions which also assumes, among others, insulation enhancement of the ground floor. For the middle PF comparison, which refers to the energy system selection and sizing, the marker shapes represent the different energy systems to be installed and the marker colors represent the capacity of the installed systems. We observe a perfect matching of the energy systems selected and very good accuracy of the capacity of the recommended systems. For instance, for

the CO_2 - optimal solution, the target biomass boiler's capacity is 16.17 kW and the predicted capacity is 15.49 kW . More specifically, for the cost-optimal solutions ASHP is selected, followed by GSHP and then again ASHP as we move towards the CO_2 optimal solutions were biomass boilers are preferred. Concerning the right-hand side PF comparison, the different marker shapes represent the different selection among renewable energy technologies and type of storage system to be installed. Similarly, we observe a good matching between the predicted and the target values. The only differences are observed when the target solution is to install PV and thermal storage and the prediction is to also install solar thermal collectors. In respect to the prediction of the objective values, the total costs and the CO_2 emissions, is accurate with an error of $0.54 \text{ CHF/m}^2/\text{a}$ and $0.25 \text{ kg CO}_2/\text{m}^2/\text{a}$, respectively. Finally, it should be mentioned that there is a triplicated optimal solution for PFP4 for PF of the CRP while the surrogate retrofit model leads to nine PF solutions since one is cut-off from the Pareto dominant filter.

In Fig. 10, the same comparison plots are depicted for a SFH built between 1919 and 1948 with a total floor area of 139.7 m^2 and a height of 10.5 m . The SFH is also heated with a gas boiler. Similarly to the MFH, we observe a very good matching on the building envelope interventions and the system selection and sizing. A good matching is also observed for the selection of renewable energy technologies and the storage system to be installed. The performance on the prediction of the objective values is slightly worse with a deviation from the target values of $1.32 \text{ CHF/m}^2/\text{a}$ and $0.71 \text{ kg CO}_2/\text{m}^2/\text{a}$, respectively.

Another functionality of the surrogate models, as already described, is the prediction of the capacity of the installed renewable energy systems and their respective storage capacity. In Fig. 11, the performance of the surrogate model in predicting renewable energy system and storage capacity for the cost-optimal, the CO_2 optimal and the PFP5 solutions for the abovementioned MFH and SFH is depicted with the use of radar plots. Each of the axes represent the four capacities to be predicted; the PV, the solar thermal collector, the thermal storage and the electrical storage. It should be mentioned that the capacity of the renewable energy technologies is measured in m^2 of covered roof area, while the storage capacity is measured in kW . The different colors represent the different PFPs' solutions, the dotted lines represent the outputs of the surrogate model, while the solid lines represent the output of the CRP for comparison purposes.

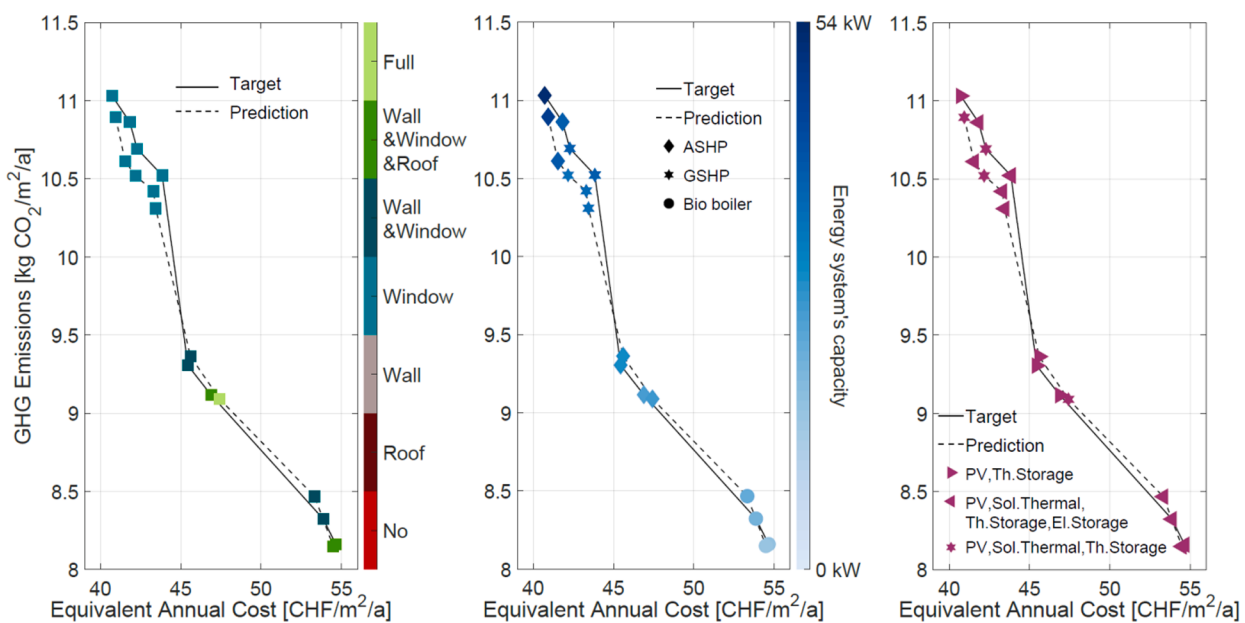


Fig. 9. Prediction of building envelope interventions (left), energy systems' selection and sizing (middle) and renewable technologies and storage selection (right) for a multi-family house built between 1919 and 1948. Solid lines represent the output of the conventional retrofit process while the dotted lines represent the outputs of the proposed surrogate model.

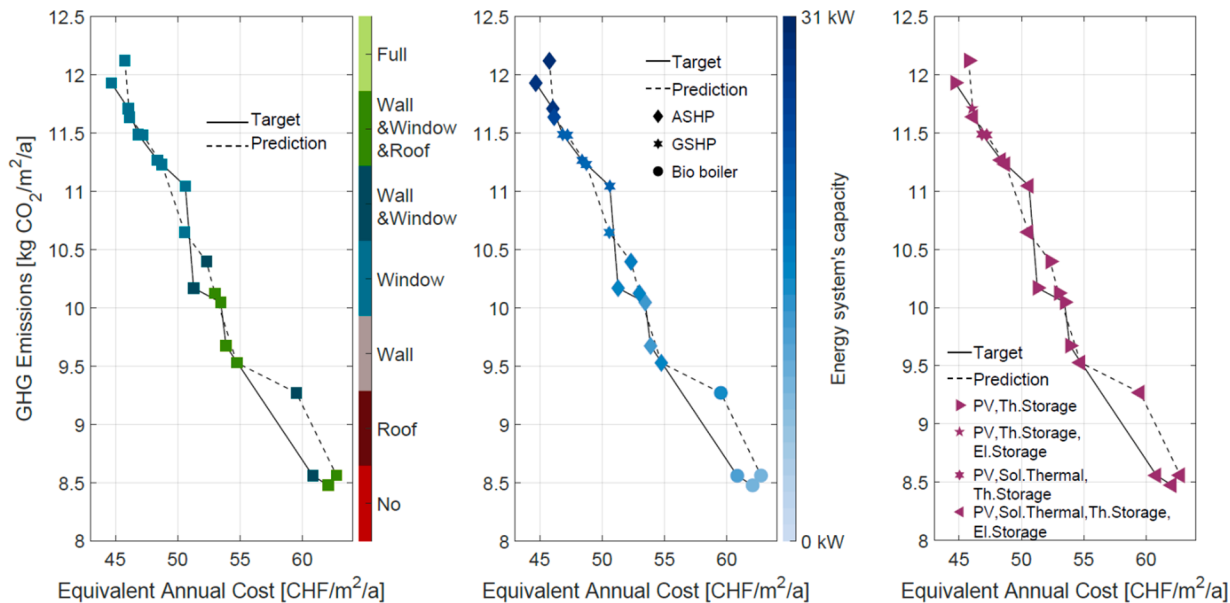


Fig. 10. Prediction of building envelope interventions (left), energy systems' selection and sizing (middle) and renewable technologies and storage selection (right) for a single-family house built between 1919 and 1948. Solid lines represent the output of the conventional retrofit process while the dotted lines represent the outputs of the proposed surrogate model.

The left-hand side radar plot, represents the predictions for the MFH already introduced, with an assumed roof area of 262.2 m² and a roof inclination of 43.7°. We can observe an accurate prediction for the PFP5 for all the four plot dimensions. The same applies for the CO₂ optimal solution, except of the PV capacity prediction in which we can observe a deviation of almost 9 m². For the cost-optimal solution, we can observe that the retrofit surrogate model correctly suggests not to install any electrical storage, but as also seen in the right-hand side plot of Fig. 9, it suggests the installation of thermal storage with almost 3kW. There is, also, a deviation on the PV capacity and the thermal storage capacity of almost 15 m² and 13 kW, respectively.

On the right-hand side radar plot of Fig. 11, the results for the SFH, with an assumed roof area of 181.1 m² and a roof inclination of 39.5°, are illustrated. With respect to the PV capacity, for all the given solutions we observe a deviation from 6.9 m² in the PFP 5 to 13.7 m², in the cost-optimal solution. In regards to the solar thermal collector capacity, a maximum deviation of 1.2 m² in the PFP5 solution can be observed. Concerning the thermal storage, the deviation varies from 3 kW, in the CO₂ optimal solution, to 13.6 kW in the cost-optimal solution. Lastly, for the electrical storage we observe a maximum deviation of 4.5 kW in the PFP5 solution.

To sum up, from both radar plots we can detect that almost all the roof area is exploited to install PVs for the cost-optimal solution, while some of the roof area is given to install solar thermal collectors for the CO₂ optimal solution. Moreover, since batteries are quite expensive to be installed electrical storage is suggested when moving towards the CO₂ optimal solutions.

4.3. Advantages and limitations of the surrogate model

The abovementioned results are very promising, especially if we also account the benefits of using such a surrogate model instead of the building-optimization building retrofit approaches. Indeed, the accuracy of the surrogate model is not as high as the CRP, yet the benefits obtained have the potential to outweigh that reduction. Two key advantages compared to the CRP is its computational efficiency and the ease of application.

The use of a small set of already known, or easily accessible, building input data and the fact that there is no need to set any parameters, after the surrogate model is trained, has the potential to make the surrogate model more accessible and convenient to use by non-expert people. For instance, there is no need to provide as input to the model the building

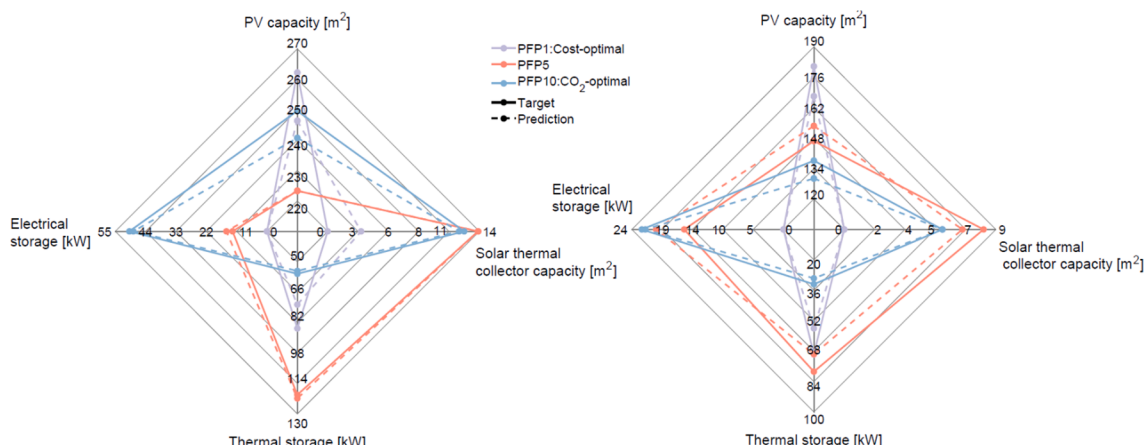


Fig. 11. Prediction of renewable energy system and storage capacity for the cost-optimal, the CO₂ optimal and the PFP5 solutions for a multi-family (left) and a single-family (right) house.

envelope intervention costs and embodied emissions since those are learnt during the training process. Moreover, it can produce the PF solutions independently based on the user's requirements. Finally, the running retrofit selection time is being drastically reduced from approximately 3.5 min to 16.4 μsec in an Intel Xeon CPU E5-2680 running at 2.50 GHz, when compared to the CRP.

Although this reduction might not be valuable for the case of a single building, it is of high importance in the scenario of having to retrofit a portfolio composed of multiple buildings. Indeed, the principled generalization ability of the proposed surrogate retrofit model makes the model capable of transferring existing knowledge from one building to another. More specifically, the developed model can be applied to other residential buildings without having to re-adjust the model to derive near-optimal retrofit solutions. One of the limitations of the model, is that it can only be used for residential buildings and only for buildings of the city of Zurich. However, the model could potentially be used for a different city. This hypothesis is valid if and only if the selected buildings' data from the other city are from the same continuous distribution of the building data selected in this work. This can be proved with the use of the Kolmogorov-Smirnov test applied in [Section 2](#).

4.4. Comparison with existing machine learning retrofit models

A direct comparison of the proposed surrogate model with other existing retrofit models is not straightforward. As already mentioned, there exist several engineering models for building retrofit in addition to the CRP used in this work. The majority of those use GAs to implement the optimization part of the building retrofit process. GAs cannot ensure the global optimality of the obtained solutions, while the MILP optimization used in the CRP can ensure the global optimality of the derived solutions.

Apart from the engineering approaches there exist also machine learning approaches. In most of them, the optimization is still performed by GAs. Machine learning is exploited for the building simulation part, or in other words to predict the energy demand profiles necessary for the different retrofit scenarios. A quantitative comparison between those models and the proposed surrogate model has certain obstacles. Firstly, the results of this work are case specific and thus cannot be compared to results of other case studies. Secondly, each retrofit study usually sets different objectives and thus a direct comparison is hard to be made. Finally, to the best of our knowledge none of the proposed retrofit approaches presented in the literature compare their results with the same CRP considered in this work. Thus, a direct comparison of the results is not possible.

On the other hand, there is a significant qualitative difference of the proposed surrogate model and the other ML-based models. Specifically, the proposed surrogate model replaces both the building simulation and optimization parts of the building retrofit process. This makes the developed model handier and easier to use, since, as soon as the model is trained, there is no need to adjust any parameters of the model. Moreover, the surrogate model is trained to approximate global optimal solutions while the GAs cannot ensure the global optimality of the obtained results. Finally, the model is faster and can be easily offered as a mobile application to be used as a retrofitting advisor.

5. Conclusions

In this paper, a surrogate retrofit model for predicting near-optimal retrofit solutions for residential buildings is presented in order to benefit from: (i) a good balance between computational cost and accuracy, (ii) use of already known or easily accessible input building data, (iii) reduced level of expertise needed to run it, and (iv) a base retrofit model that can be easily generalized for large-scale retrofitting analysis in wide-areas. For the training and validation of the proposed model, one of the most advanced retrofit approaches, which is based on building simulation and multi-objective optimization tools, was used.

The developed surrogate model consists of two machine learning sub-models. Artificial neural networks are used to build up those two sub-models. The first predicts the CO₂ optimal and the other predicts the rest of the Pareto front solutions. Each suggested retrofit solution pertains to the necessary building envelope interventions, the energy system replacement and sizing as well as the integration of renewable technologies and energy storage.

The case study of the city of Zurich is used to collect the necessary residential buildings' data so as to properly train and illustrate the benefits of the surrogate model. Compared to the conventional retrofit process, the proposed surrogate model has an average performance of $R^2 = 0.8789$ for the continues variables, and an average performance of $f1\ score = 0.9036$, for the categorical variables. Furthermore, the surrogate model is less expensive in calculating near-optimal retrofit solutions and, as soon as it is trained for a given city, we could argue that it can be handier for non-expert people. Those advantages are becoming more important in practical applications and when retrofit decisions for multiple buildings are desired, and the computational cost of the conventional approaches exceed the available computational resources.

There are some improvements that could be considered to enhance the performance of the surrogate model. Changes to the model architecture, e.g., using deeper artificial neural networks, residual connections, use of more advanced methods to define the structure of the model, e.g., neural architecture search techniques, and testing of other machine learning algorithms, such as random forests, to improve the model interpretability, are some of them. A further option for future work would be to check the confidence of the model so that its predictions would be rejected in case of an outlier building.

Finally, this surrogate model can be further enhanced in order to be used for retrofit analysis at wide-areas, from neighborhoods, cities and communities. More specifically, an equivalent surrogate model that accounts for the regional variability can be trained and used to predict retrofit solutions at various regions. Towards that direction, transfer learning could be exploited by making use of the knowledge gained from the proposed surrogate model so as to easier and with less samples train another model that could be applied to buildings in whole Switzerland. In that way, the full potential of such surrogate models could be exploited in order to enable more computationally efficient methods for large-scale building retrofit planning.

CRediT authorship contribution statement

Emmanouil Thrampoulidis: Conceptualization, Methodology, Software, Formal analysis, Investigation, Visualization, Writing - original draft. **Georgios Mavromatidis:** Conceptualization, Resources, Writing - review & editing, Supervision. **Aurelien Lucchi:** Conceptualization, Writing - review & editing. **Kristina Orehounig:** Writing - review & editing, Supervision, Project administration, Funding acquisition.

Declaration of Competing Interest

The authors declare that they have no known competing financial interests or personal relationships that could have appeared to influence the work reported in this paper.

Acknowledgements

This research project is financially supported by the Swiss Innovation Agency Innosuisse and is part of the Swiss Competence Center for Energy Research SCCER FEEB&D.

Appendix A

See [Tables A1–A4](#).

Table A1
Energy Hub model's parameters.

Cost parameters	Operating costs	Grid (electricity) (<i>CHF/kWh</i>)	0.304
		Gas boiler (<i>CHF/kWh</i>)	0.1455
		Oil boiler (<i>CHF/kWh</i>)	0.135
		Bio boiler (<i>CHF/kWh</i>)	0.146
		District heating (existing) (<i>CHF/kWh</i>)	0.120
	Linear Capital costs	ASHP (<i>CHF/kW</i>)	1020
		GSHP (<i>CHF/kW</i>)	2380
		Gas boiler (<i>CHF/kW</i>)	620
		Oil boiler (<i>CHF/kW</i>)	570
		Bio boiler (<i>CHF/kW</i>)	860
		Solar thermal collector (<i>CHF/m²</i>)	1000
		Electricity (existing) (<i>CHF/kW</i>)	100
		Photovoltaics (<i>CHF/m²</i>)	400
		District heating (existing) (<i>CHF/kW</i>)	75
		Floor heating (<i>CHF/m²</i>)	100
	Fixed Capital costs	Thermal storage (<i>CHF/kW</i>)	12.5
		Electrical storage (<i>CHF/kW</i>)	2000
		ASHP (<i>CHF</i>)	18300
		GSHP (<i>CHF</i>)	20000
		Gas boiler (<i>CHF</i>)	27600
Lifetime Parameters		Oil boiler (<i>CHF</i>)	26600
		Bio boiler (<i>CHF</i>)	27800
		Solar thermal collector (<i>CHF</i>)	4000
Emission Parameters	Carbon factors	Electricity (existing) (<i>CHF</i>)	100
		Photovoltaics (<i>CHF</i>)	900
		Heat Pump (existing) (<i>CHF</i>)	9150
		Thermal storage (<i>CHF</i>)	1685
	Boreholes (years)	Boreholes (years)	50
		Floor heating (years)	25
		Retrofit (years)	50
	Linear embodied emissions	Grid (<i>kg CO₂/kWh</i>)	0.1369
		Gas boiler (<i>kg CO₂/kWh</i>)	0.228
		Oil boiler (<i>kg CO₂/kWh</i>)	0.301
		Bio boiler (<i>kg CO₂/kWh</i>)	0.027
		CHP (<i>kg CO₂/kWh</i>)	0.228
		District Heating (existing) (<i>kg CO₂/kWh</i>)	0.089
		Floor Heating (<i>kg CO₂/m²</i>)	5.06
		ASHP (<i>kg CO₂/kWh</i>)	74.760
		GSHP (<i>kg CO₂/kWh</i>)	72.270
		Gas boiler (<i>kg CO₂/kWh</i>)	51.2
Fixed embodied emissions		Oil Boiler (<i>kg CO₂/kWh</i>)	51.2
		Bio boiler (<i>kg CO₂/kWh</i>)	51.2
		CHP (<i>kg CO₂/kWh</i>)	4000
		Photovoltaics (<i>kg CO₂/m²</i>)	253.75
		Solar thermal collector (<i>kg CO₂/m²</i>)	184
		District heating (existing) (<i>kg CO₂/kWh</i>)	25.8
		Electricity (existing) (<i>kg CO₂/kWh</i>)	25.8
		Boreholes (<i>kg CO₂/m</i>)	28.1
		Thermal storage (<i>kg CO₂/kW</i>)	4.68
		El. storage (<i>kg CO₂/kW</i>)	157.14
	Thermal storage (<i>kg CO₂</i>)	ASHP (<i>kg CO₂</i>)	2329.3
		GSHP (<i>kg CO₂</i>)	1806.2
		Thermal storage (<i>kg CO₂</i>)	30.690

Table A2

Embodied emission values for retrofitting.

Component/Material	Density (kg/m ³)	Embodied GHG
Expanded polystyrene (EPS)	27.5	7.53 [kgCO ₂ /kg]
Glazing	–	57.6 [kgCO ₂ /m ²]

Table A3

Embodied emission values for energy systems and storage.

System	GHG factor (kgCO ₂ /kW)	GHG factor (kgCO ₂ /m ²)	GHG factor (kgCO ₂ /kWh)
Boiler	51.2	–	–
ASHP	74.76 [+2329.3 (fixed)]	–	–
GSHP	72.27 [+1806.2 (fixed)]	–	–
Boreholes	0.803	–	–
PV	–	253.75	–
Solar thermal collector	–	184	–
Floor heating	–	5.06	–
Electrical Storage ¹	–	–	157.14
Thermal storage ²	–	–	4.68 [+30.69 (fixed)]

¹ Lithium batteries were considered as electrical energy storage.² Water tanks, with an assumed temperature difference between the water and the ambient temperature of ΔT = 35 °C, were selected as thermal energy storage.**Table A4**

Efficiency of considered energy systems.

Energy system	Efficiency
ASHP	3
GSHP	4
Gas boiler	0.9
Oil boiler	0.9
Bio boiler	0.85
Solar thermal collector	0.45
Electricity (existing)	1
Photovoltaics	0.15
District heating (existing)	0.95
Heat pump (existing)	2
Gas boiler (existing)	0.8
Oil boiler (existing)	0.8
Bio boiler (existing)	0.75

Appendix B

See Figs. B1 and B2.

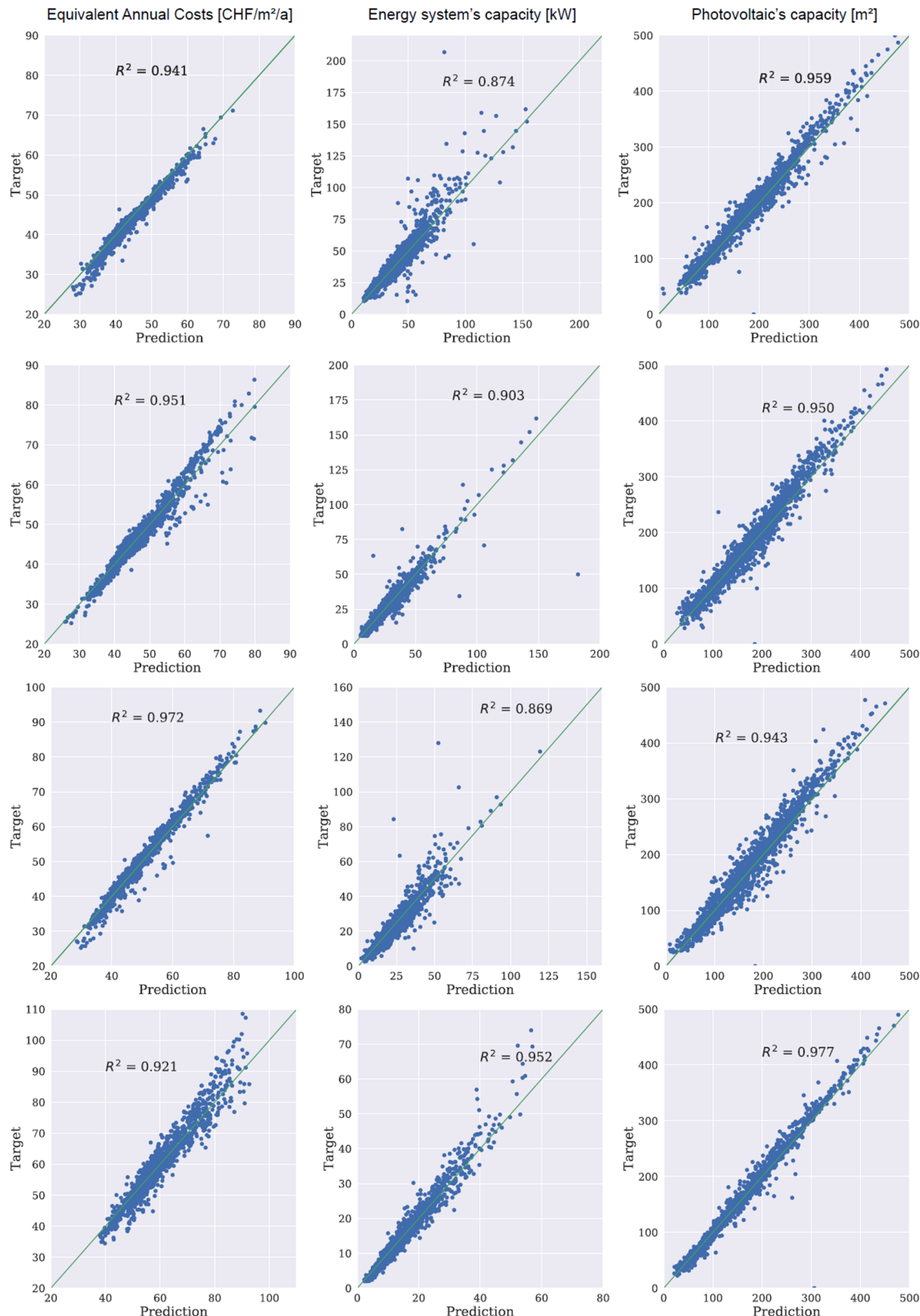


Fig. B1. Prediction performance of the surrogate model on a test set of residential buildings. Regression plots for PFP2 (first row), PFP5 (second row), PFP 7 (third row) and PFP10: CO₂ – optimal solution (last row).



Fig. B2. Prediction performance of the surrogate model on a test set of residential buildings. Confusion matrices for PFP2 (first row), PFP5 (second row), PFP 7 (third row) and PFP10: CO₂ – optimal solution (last row).

References

- [1] European Commission. Energy performance of buildings. Energy - European Commission; 2014. <https://ec.europa.eu/energy/en/topics/energy-efficiency/energy-performance-of-buildings/overview> (accessed January 13, 2020).
- [2] SFOE, Swiss Federal Office of Energy. Measures for increasing energy efficiency. <https://www.bfe.admin.ch/bfe/en/home/politik/energiestrategie-2050/erstes-massnahmenpaket/massnahmen-zur-steigerung-der-energieeffizienz.html> (accessed January 13, 2020).
- [3] BFE, Bundesamt für Energie. Energieperspektiven 2050 <https://www.bfe.admin.ch/bfe/de/home/politik/energiestrategie-2050/dokumentation/energieperspektiven-2050.html> (accessed January 13, 2020).
- [4] Directive 2010/31/EU of the European Parliament and of the Council of 19 May 2010 on the energy performance of buildings OJ L 153 2010.
- [5] Directive 2012/27/EU of the European Parliament and of the Council of 25 October 2012 on energy efficiency, amending Directives 2009/125/EC and 2010/30/EU and repealing Directives 2004/8/EC and 2006/32/EC Text with EEA relevance 2012.
- [6] Directive (EU) 2018/844 of the European Parliament and of the Council of 30 May 2018 amending Directive 2010/31/EU on the energy performance of buildings and Directive 2012/27/EU on energy efficiency (Text with EEA relevance) 2018;156.
- [7] EU low energy standards confirmed for 2020 building regulations. <https://www.current-news.co.uk/news/eu-low-energy-standards-confirmed-for-2020-building-regulations> (accessed January 13, 2020).
- [8] Nino Streicher K, Parra D, Buerer MC, Patel MK. Techno-economic potential of large-scale energy retrofit in the Swiss residential building stock. *Energy Procedia* 2017;122:121–6. <https://doi.org/10.1016/j.egypro.2017.07.314>.
- [9] Nielsen AN, Jensen RL, Larsen TS, Nissen SB. Early stage decision support for sustainable building renovation – A review. *Build Environ* 2016;103:165–81. <https://doi.org/10.1016/j.buildenv.2016.04.009>.
- [10] Ma Z, Cooper P, Daly D, Ledo L. Existing building retrofits: methodology and state-of-the-art. *Energy Build* 2012;55:889–902. <https://doi.org/10.1016/j.build.2012.08.018>.
- [11] Hsu D. How much information disclosure of building energy performance is necessary? *Energy Policy* 2014;64:263–72. <https://doi.org/10.1016/j.enpol.2013.08.094>.
- [12] Ceballos-Fuentealba I, Álvarez-Miranda E, Torres-Fuchslocher C, del Campo-Hitschfeld ML, Díaz-Guerrero J. A simulation and optimisation methodology for choosing energy efficiency measures in non-residential buildings. *Appl Energy* 2019;256:113953. <https://doi.org/10.1016/j.apenergy.2019.113953>.
- [13] Mora TD, Righi A, Peron F, Romagnoni P. Cost-Optimal measures for renovation of existing school buildings towards nZEB. *Energy Procedia* 2017;140:288–302. <https://doi.org/10.1016/j.egypro.2017.11.143>.
- [14] Fan Y, Xia X. A multi-objective optimization model for energy-efficiency building envelope retrofitting plan with rooftop PV system installation and maintenance. *Appl Energy* 2017;189:327–35. <https://doi.org/10.1016/j.apenergy.2016.12.077>.
- [15] Ascione F, Bianco N, da Silva MG, Antunes CH, Dias L, Glicksman L. Multi-objective optimization for building retrofit: A model using genetic algorithm and artificial neural network and an application. *Energy Build* 2014;81:444–56. <https://doi.org/10.1016/j.build.2014.11.058>.
- [16] Ascione F, Bianco N, Mauro GM, Napolitano DF. Retrofit of villas on Mediterranean coastlines: Pareto optimization with a view to energy-efficiency and cost-effectiveness. *Appl Energy* 2019;254:113705. <https://doi.org/10.1016/j.apenergy.2019.113705>.
- [17] Niemelä T, Kosonen R, Jokisalo J. Energy performance and environmental impact analysis of cost-optimal renovation solutions of large panel apartment buildings in Finland. *Sustain Cities Soc* 2017;32:9–30. <https://doi.org/10.1016/j.scs.2017.02.017>.
- [18] Juan Y-K, Kim JH, Roper K, Castro-Lacouture D. GA-based decision support system for housing condition assessment and refurbishment strategies. *Autom Constr* 2009;18:394–401. <https://doi.org/10.1016/j.autcon.2008.10.006>.
- [19] Mavromatidis G. Model-based design of distributed urban energy systems under uncertainty. Doctoral Thesis. ETH Zurich; 2017. <https://doi.org/10.3929/ethz-b-000182697>.
- [20] Wu R, Mavromatidis G, Orehoung K, Carmeliet J. Multiobjective optimisation of energy systems and building envelope retrofit in a residential community. *Appl Energy* 2017;190:634–49. <https://doi.org/10.1016/j.apenergy.2016.12.161>.
- [21] Winston P. 6.034 Artificial Intelligence. Massachusetts Institute of Technology: MIT OpenCourseWare; 2010.
- [22] Wang D, Landolt J, Mavromatidis G, Orehoung K, Carmeliet J. CESAR: a bottom-up building stock modelling tool for Switzerland to address sustainable energy transformation strategies. *Energy Build* 2018;169:9–26. <https://doi.org/10.1016/j.build.2018.03.020>.
- [23] Geidl M, Koeppl G, Favre-Perrod P, Klockl B, Andersson G, Frohlich K. Energy hubs for the future. *IEEE Power Energy Mag* 2007;5:24–30. <https://doi.org/10.1109/MPAE.2007.264850>.
- [24] Rogeau A, Girard R, Abdelouadoud Y, Thorel M, Kariniotakis G. Joint optimization of building-envelope and heating-system retrofits at territory scale to enhance decision-aiding. *Appl Energy* 2020;264:114639. <https://doi.org/10.1016/j.apenergy.2020.114639>.
- [25] Costa-Carrapico I, Raslan R, González JN. A systematic review of genetic algorithm-based multi-objective optimisation for building retrofitting strategies towards energy efficiency. *Energy Build* 2020;210:109690. <https://doi.org/10.1016/j.build.2019.109690>.
- [26] Hashempour N, Taherkhani R, Mahdikhani M. Energy performance optimization of existing buildings: a literature review. *Sustain Cities Soc* 2020;54:101967. <https://doi.org/10.1016/j.scs.2019.101967>.
- [27] Bourdeau M, Zhai X qiang, Neffzoui E, Guo X, Chatellier P. Modeling and forecasting building energy consumption: a review of data-driven techniques. *Sustain Cities Soc* 2019;48:101533. <https://doi.org/10.1016/j.scs.2019.101533>.
- [28] Voyant C, Notton G, Darras C, Fouillot A, Motte F. Uncertainties in global radiation time series forecasting using machine learning: the multilayer perceptron case. *Energy* 2017;125:248–57. <https://doi.org/10.1016/j.energy.2017.02.098>.
- [29] Wang H, Li G, Wang G, Peng J, Jiang H, Liu Y. Deep learning based ensemble approach for probabilistic wind power forecasting. *Appl Energy* 2017;188:56–70. <https://doi.org/10.1016/j.apenergy.2016.11.111>.
- [30] Van Every PM, Rodriguez M, Jones CB, Mammoli AA, Martínez-Ramón M. Advanced detection of HVAC faults using unsupervised SVM novelty detection and Gaussian process models. *Energy Build* 2017;149:216–24. <https://doi.org/10.1016/j.enbuild.2017.05.053>.
- [31] Mavromatidis G, Acha S, Shah N. Diagnostic tools of energy performance for supermarkets using Artificial Neural Network algorithms. *Energy Build* 2013;62:304–14. <https://doi.org/10.1016/j.enbuild.2013.03.020>.
- [32] Papadimitriou T, Gogas P, Stathakis E. Forecasting energy markets using support vector machines. *Energy Econ* 2014;44:135–42. <https://doi.org/10.1016/j.eneco.2014.03.017>.
- [33] Yu L, Zhao Y, Tang L. A compressed sensing based AI learning paradigm for crude oil price forecasting. *Energy Econ* 2014;46:236–45. <https://doi.org/10.1016/j.eneco.2014.09.019>.
- [34] Mosavi A, Salimi M, Faizollahzadeh Ardabili S, Rabczuk T, Shamshirband S, Varkonyi-Koczy AR. State of the art of machine learning models in energy systems, a systematic review. *Energies* 2019;12:1301. <https://doi.org/10.3390/en12071301>.
- [35] Georgiou GS, Christodoulides P, Kalogirou SA. Implementing artificial neural networks in energy building applications — A review. 2018 IEEE Int. Energy Conf. ENERGYCON, 2018, p. 1–6. <https://doi.org/10.1109/ENERGYCON.2018.8398847>.
- [36] Marasca DE, Kontokosta CE. Applications of machine learning methods to identifying and predicting building retrofit opportunities. *Energy Build* 2016;128:431–41. <https://doi.org/10.1016/j.enbuild.2016.06.092>.
- [37] Magnier L, Haghifat H. Multiobjective optimization of building design using TRNSYS simulations, genetic algorithm, and Artificial Neural Network. *Build Environ* 2010;45:739–46. <https://doi.org/10.1016/j.buildenv.2009.08.016>.
- [38] Asadi E, da Silva MG, Antunes CH, Dias L, Glicksman L. Multi-objective optimization for building retrofit: A model using genetic algorithm and artificial neural network and an application. *Energy Build* 2014;81:444–56. <https://doi.org/10.1016/j.enbuild.2014.04.009>.
- [39] Ascione F, Bianco N, De Stasio C, Mauro GM, Vanoli GP. CASA, cost-optimal analysis by multi-objective optimisation and artificial neural networks: a new framework for the robust assessment of cost-optimal energy retrofit, feasible for any building. *Energy Build* 2017;146:200–19. <https://doi.org/10.1016/j.enbuild.2017.04.069>.
- [40] Prada A, Gasparella A, Baggio P. On the performance of meta-models in building design optimization. *Appl Energy* 2018;225:814–26. <https://doi.org/10.1016/j.apenergy.2018.04.129>.
- [41] Gilan SS, Dilkina BN. Sustainable Building Design: A Challenge at the Intersection of Machine Learning and Design Optimization. AAAI Workshop Comput. Sustain., 2015.
- [42] Yuan J, Nian V, Su B. Evaluation of cost-effective building retrofit strategies through soft-linking a metamodel-based Bayesian method and a life cycle cost analysis method. *Appl Energy* 2019;253:113573. <https://doi.org/10.1016/j.apenergy.2019.113573>.
- [43] Tian Z, Zhang X, Jin X, Zhou X, Si B, Shi X. Towards adoption of building energy simulation and optimization for passive building design: a survey and a review. *Energy Build* 2017;158. <https://doi.org/10.1016/j.enbuild.2017.11.022>.
- [44] Lee SH, Hong T, Piette MA, Taylor-Lange SC. Energy retrofit analysis toolkits for commercial buildings: a review. *Energy* 2015;89:1087–100. <https://doi.org/10.1016/j.energy.2015.06.112>.
- [45] Wu Z, Wang B, Xia X. Large-scale building energy efficiency retrofit: concept, model and control. *Energy* 2016;109:456–65. <https://doi.org/10.1016/j.energy.2016.04.124>.
- [46] Bundesamt für Statistik. Gebäude Und Wohnungsregister 2013.
- [47] 3D-Stadtmodell - Stadt Zürich https://www.stadt-zuerich.ch/ted/de/index/geoz/geodaten_u_plaene/3d_stadtmodell.html (accessed April 17, 2020).
- [48] GEAK. <https://www.geak.ch/> (accessed April 9, 2020).
- [49] KBOB K der BL der öffentlichen B. Ökobilanzdaten im Baubereich 2009/1:2016 https://www.kbob.admin.ch/kbob/de/home/publikationen/nachhaltiges-bauen/oekbilanzdaten_baubereich.html (accessed April 9, 2020).
- [50] DesignBuilder Software Ltd - Home <https://designbuilder.co.uk/> (accessed April 8, 2020).
- [51] GEAK® | Gebäudeenergieausweis der Kantone. <http://geak.ch/> (accessed February 12, 2018).
- [52] Hiremath M, Derendorf K, Vogt T. Comparative life cycle assessment of battery storage systems for stationary applications. *Environ Sci Technol* 2015;49. <https://doi.org/10.1021/es504572q>.
- [53] Mavromatidis G, Orehoung K, Carmeliet J. Evaluation of photovoltaic integration potential in a village. *Sol Energy* 2015;121. <https://doi.org/10.1016/j.solener.2015.03.044>.
- [54] Klingler M, Kasser U, Savi D, Primas A, Stettler Y. Ökobilanzdaten für Lüftungs- und Wärmeanlagen; Sach- und Ökobilanzen von sechzehn verschiedenen

- Gebäuden in den Bereichen Wohnen, Büro, Schulen und Altersheime - Schlussbericht (Ökobilanzdaten für Lüftungs- und Wärmeanlagen; Sach- und Ökobilanzen von sechzehn verschiedenen Gebäuden in den Bereichen Wohnen, Büro, Schulen und Altersheime - Schlussbericht). Energy Build 2014.
- [55] Umweltauswirkungen von Schweizer Strommixen - Stadt Zürich. <https://www.adt-zuerich.ch/hbd/de/index/hochbau/bauen-fuer-2000-watt/grundlagen-studienergebnisse/archiv-studien/2013/2013-04-nb-life-cycle-electricity.html> (accessed February 12, 2018).
- [56] Murray P, Marquant J, Niffeler M, Mavromatis G, Orehoung K. Optimal transformation strategies for buildings, neighbourhoods and districts to reach CO₂ emission reduction targets. Energy Build 2020;207:109569. <https://doi.org/10.1016/j.enbuild.2019.109569>.
- [57] Mavromatis G, Evans R, Orehoung K, Dorer V, Carmeliet J. Multi-objective optimization to simultaneously address energy hub layout, sizing and scheduling using a linear formulation. Eng Optim IV Present Int Conf Eng Optim 2014:609–14. <https://doi.org/10.1201/b17488-108>.
- [58] Liu FT, Ting KM, Zhou Z. Isolation Forest. In: 2008 Eighth IEEE Int. Conf. Data Min., 2008, p. 413–22. <https://doi.org/10.1109/ICDM.2008.17>.
- [59] 6.3. Preprocessing data — scikit-learn 0.22.2 documentation. <https://scikit-learn.org/stable/modules/preprocessing.html> (accessed April 9, 2020).
- [60] Thrampoulidis E, Mavromatis G, Orehoung K, Carmeliet J. Emulation of energy optimization models via machine learning towards retrofitting existing buildings, 20th Brenet Status-Seminar, Zurich: 2018.
- [61] Kalogirou SA. Artificial neural networks in renewable energy systems applications: a review. Renew Sustain Energy Rev 2001;5:373–401. [https://doi.org/10.1016/S1364-0321\(01\)00006-5](https://doi.org/10.1016/S1364-0321(01)00006-5).
- [62] Goodfellow I, Bengio Y, Courville A. Deep learning. MIT Press; 2016.
- [63] Kingma DP, Ba J. Adam: A Method for Stochastic Optimization. ArXiv14126980 Cs; 2014.
- [64] Chollet, Francois. Keras; 2015. <https://keras.io/> (accessed February 25, 2019).
- [65] TensorBoard: Visualizing Learning | TensorFlow https://www.tensorflow.org/guide/summaries_and_tensorboard (accessed February 25, 2019).